Inorganic Chemistry
Cite This: Inorg. Chem. 2019, 58, 3724−3731
Article
pubs.acs.org/IC

Protonation Studies of Molybdenum(VI) Nitride Complexes That Contain the $[2,6\text{-}(ArNCH_2)_2NC_5H_3]^{2-}$ Ligand (Ar = 2,6-Diisopropylphenyl)

Anne K. Hickey, Lasantha A. Wickramasinghe, Richard R. Schrock,* Charlene Tsay, and Peter Müller

Department of Chemistry, Massachusetts Institute of Technology, 77 Massachusetts Avenue, Cambridge, Massachusetts 02139, United States

Supporting Information

ABSTRACT: $[Ar_2N_3]Mo(N)(O\text{-}t\text{-}Bu)$ (**1**), which contains the conformationally rigid pyridine-based diamido ligand $[2,6\text{-}(ArNCH_2)_2NC_5H_3]^{2-}$ (Ar = 2,6-diisopropylphenyl), is a catalyst for the reduction of dinitrogen with protons and electrons. Various acids have been added in order to explore where and how the first proton adds to the complex. The addition of adamantol to **1** produces a five-coordinate bis(adamantoxide), $[HAr_2N_3]Mo(N)(OAd)_2$ (**2a**), in which one of the amido nitrogens in the ligand has been protonated and the resulting aniline nitrogen in the $[HAr_2N_3]^-$ ligand is not bound to the metal. The addition of $[Ph_2NH_2][OTf]$ to **1** produces $\{[HAr_2N_3]Mo(N)(O\text{-}t\text{-}Bu)\}(OTf)$ (**3**), in which an amido nitrogen has been protonated, but the aniline in the $[HAr_2N_3]^-$ ligand remains *bound* to the metal. Last, the addition of (2,6-lutidinium)BAr^F_4 (BAr^F_4 = $\{B(3,5\text{-}(CF_3)_2C_6H_3)_4\}^-$) to **1** yields $\{[Ar_2N_3]Mo(N)(LutH)(O\text{-}t\text{-}Bu)\}BAr^F_4$, in which $LutH^+$ is hydrogen-bonded to the nitride in the solid state and in dichloromethane with K_{eq} = 412 ± 94 and ΔG = −3.6 ± 0.8 kcal at 22 °C. A similar hydrogen-bonded adduct was formed through the addition of (2-methylpyridinium)BAr^F_4 to **1**, but the addition of (pyridinium)BAr^F_4 to **1** leads to the formation of (inter alia) $\{[HAr_2N_3]Mo(N)(O\text{-}t\text{-}Bu)\}(BAr^F_4)$, in which the amide nitrogen has been protonated. The addition of cobaltocene to **3** or $\{[Ar_2N_3]Mo(N)(LutH)(O\text{-}t\text{-}Bu)\}(BAr^F_4)$ leads only to the re-formation of **1**. X-ray structural studies were carried out on **2a**, **3**, and $\{[Ar_2N_3]Mo(N)(LutH)(O\text{-}t\text{-}Bu)\}(BAr^F_4)$.

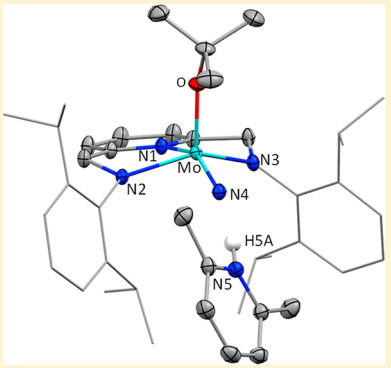

INTRODUCTION

The homogeneous catalytic reduction of molecular nitrogen to ammonia with protons and electrons under mild conditions is most efficiently carried out with catalysts that contain molybdenum,[1,2] iron,[3] or osmium.[4] The reducing agent is usually a metallocene or KC_8, and the proton source is often the $[B(3,5\text{-}(CF_3)_2C_6H_3)_4]^-$ ($BAr^F_4{}^-$) or triflate salt of some protonated nitrogen base such as a lutidinium or diphenylammonium. A minimum of six protons and six electrons must be added through linear- or side-on-bound N_xH_y intermediates in order to form ammonia. The alternative product is molecular hydrogen. Molybdenum-based catalysts can achieve high-efficiency (>90%) conversion with respect to the equivalents of reductant added.[5a] "Simpler" mechanisms of dinitrogen reduction have also been proposed, in which nitrogen is first cleaved bimolecularly into two nitrides through the formation of a μ-N_2 intermediate or intermediates.[5] This "cleavage" mechanism avoids some of the problems associated with the initial reduction or protonation of a molecular nitrogen complex, followed by the further addition of protons and electrons to N_xH_y intermediates. All in all, the homogeneous reduction of molecular nitrogen with protons and electrons in an efficient manner (ideally without the formation of hydrogen) and with high turnover numbers is one of the most challenging catalytic reactions today. Electrocatalytic reductions (homogeneous or heterogeneous) may ultimately prove to be more efficient,[6] although much research remains to be done.[7] Nitride intermediates are featured in the homogeneous "distal" and "cleavage" mechanisms.

A key issue in catalytic reduction is keeping the basic structure of the catalyst intact, i.e., avoiding side reactions such as ligand protonation that can lead to loss of ligand and loss of function. Therefore, we were surprised to find that $[Ar_2N_3]Mo(N)(O\text{-}t\text{-}Bu)$ (**1**), which contains the conformationally rigid pyridine-based tridentate diamido ligand $[2,6\text{-}(ArNCH_2)_2NC_5H_3]^{2-}$ (Ar = 2,6-diisopropylphenyl), serves as a catalyst or catalyst precursor for the catalytic reduction of molecular nitrogen to ammonia in diethyl ether between −78 and 22 °C in a batchwise manner, with $CoCp^*_2$ as the electron source and $[Ph_2NH_2][OTf]$ as the proton source.[8] Up to ∼10 equiv of ammonia is formed per molybdenum, with the maximum efficiency in electrons being ∼43%. We were surprised by this result in view of the presence of *tert*-butoxide and amido nitrogen ligands that could be protonated instead of the nitride ligand (initially) or other N_xH_y intermediates in a "distal" cycle that would involve nitrogen activation and reduction to give the second 1 equiv of ammonia and a nitride

Received: December 2, 2018
Published: February 26, 2019

DOI: 10.1021/acs.inorgchem.8b03346
Inorg. Chem. 2019, 58, 3724−3731

back again. It is not known whether **1** is turned into another type of compound whose integrity is maintained throughout catalytic turnover.

We decided to focus on formation of the first 1 equiv of ammonia from **1** and, even more specifically, simply on addition of the first proton to **1**. It has already been shown that **1** reacts with HCl to give $[Ar_2N_3]Mo(N)Cl$,[8] which does not yield any ammonia under the conditions chosen for catalytic reduction. Nevertheless, the reaction with HCl suggested that the *tert*-butoxide ligand may be protonated at an early stage. In this paper, we report the results of our first investigations into the protonation of **1**.

RESULTS

Protonation of Ligands. Because the addition of HCl to **1** yields $[Ar_2N_3]Mo(N)Cl$, the *tert*-butoxide oxygen would appear to be the "preferred" site of protonation in **1**.[8] However, whether *tert*-butoxide is protonated "directly" by an "acid" (HX) to give the salt $\{[Ar_2N_3]Mo(N)(HO\text{-}t\text{-}Bu)\}(X)$ or not will depend (inter alia) on whether HX is a strong acid and/or can bind to the metal through X, followed by proton migration to another atom in the primary coordination sphere. Therefore, we first explored the reaction between **1** and adamantol, a "weak" acid in water ($pK_a \sim 18$).[9]

Adamantol reacts with **1** in dichloromethane to give a single product only when 2 equiv of AdOH are added (eq 1). One

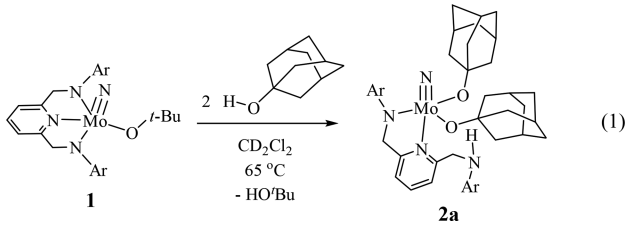

(1)

plausible scenario for formation of the bis(adamantoxide) complex **2a** is binding of the first AdOH to give $[Ar_2N_3]Mo(N)(HOAd)(O\text{-}t\text{-}Bu)$, then migration of the adamantol proton to *tert*-butoxide to give $[Ar_2N_3]Mo(N)(OAd)(HO\text{-}t\text{-}Bu)$, and finally loss of *tert*-butyl alcohol to give $[Ar_2N_3]Mo(N)(OAd)$. The addition of a second AdOH would give $[Ar_2N_3]Mo(N)(OAd)(HOAd)$. The adamantanol proton then migrates to the amide nitrogen (O to N^-) to give $[HAr_2N_3]Mo(N)(OAd)_2$ (**2a**). An earlier migration of a proton on a bound ROH to the ligand and other variations are viable options.

A partial ^1H NMR spectrum of **2a** reveals that the AB quartet observed for the "up" and "down" CH_2 protons next to the amido nitrogens of the pincer ligand in **1**[8] (Figure 1a) is replaced by a singlet at 4.77 ppm for the now essentially equivalent CH_2 protons next to the amide nitrogen, a second-order pattern at 4.50 ppm for the inequivalent (CHH′) protons in the other CH_2 group next to the aniline nitrogen, and a triplet at 4.06 ppm for the aniline NH proton (Figure 1b).

An X-ray study showed that **2a** has approximately a trigonal-bipyramidal geometry ($\tau = 0.77$)[10] with the nitride in the apical position (Figure 2). The structure could be refined only to ~10% (see the Supporting Information, SI), so the accuracies of the distances and angles (see the SI) are limited. However, the basic structure of **2a** is unambiguous.

An intermediate in the reported synthesis[8] of **1** turns out to be the *tert*-butoxide analogue of **2a**. The synthesis calls for the

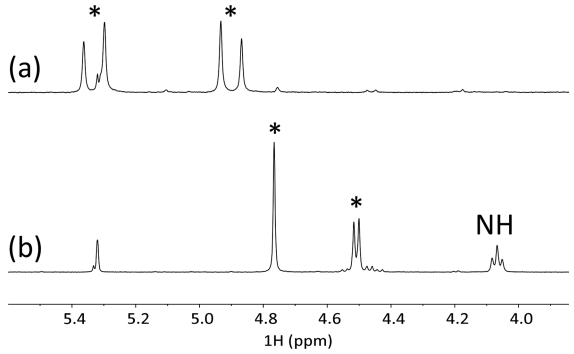

Figure 1. Partial ^1H NMR spectrum of (a) **1** and (b) **2a** showing the benzyl CH_2 resonances of the pincer ligand.

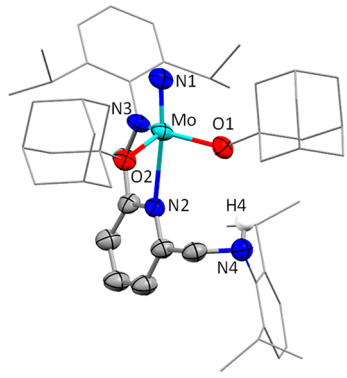

Figure 2. Structure of **2a**.

addition of 1 equiv of Li-*n*-Bu to $H_2Ar_2N_3$ in pentane to give a monolithiated ligand and then the addition of $(t\text{-}BuO)_3Mo(N)$ to give an intermediate in which only one *tert*-butoxide in the nitride has been substituted by an amido nitrogen, i.e., $[HAr_2N_3]Mo(N)(O\text{-}t\text{-}Bu)_2$ (**2b**; Scheme 1). The addition of a

Scheme 1

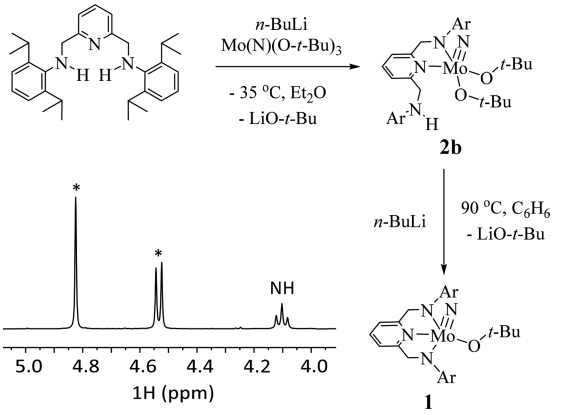

second 1 equiv of Li-*n*-Bu followed by heating of the mixture then gave **1** and a second 1 equiv of *tert*-butoxide. A partial ^1H NMR spectrum of **2b** (inset in Scheme 1) is entirely analogous to that for **2a** in Figure 1b.

A more relevant acid in terms of nitrogen reduction by **1**, as described earlier, is $[Ph_2NH_2][OTf]$.[8] The reaction between **1** and 1 equiv of $[Ph_2NH_2][OTf]$ in ether produces a yellow product that can be isolated in 60% yield ($\{[HAr_2N_3]Mo(N)(O\text{-}t\text{-}Bu)\}(OTf)$ (**3**); eq 2). An X-ray study (Figure 3)

DOI: 10.1021/acs.inorgchem.8b03346
Inorg. Chem. 2019, 58, 3724−3731

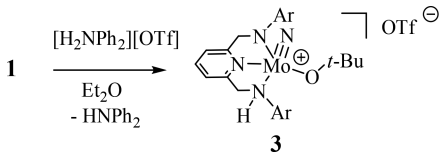

(2)

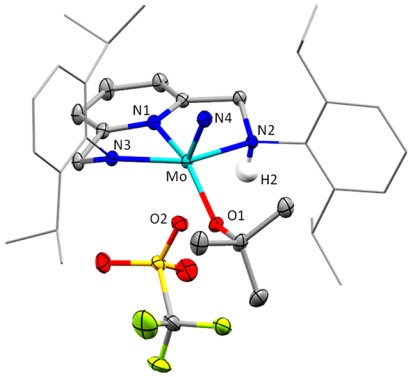

Figure 3. Molecular structure of **3**. Ellipsoids are shown at 50% probability. The aryl groups are shown as wireframes, and two cocrystallized THF molecules and hydrogen atoms except for H2 are omitted for clarity. Mo−N1 = 2.2131(11) Å, Mo−N2 = 2.2980(12) Å, Mo−N3 = 1.9673(11) Å, Mo−N4 = 1.6480(13) Å, Mo−O1 = 1.8919(10) Å, Mo−O2 = 2.65 Å, N2−Mo−N3 = 145.11(4)°, N4−Mo−O1 = 143.17(4)°, and τ = 0.03.

shows that **3** is the triflate salt of a cation that contains the $[HAr_2N_3]^-$ ligand, but the aniline nitrogen (N2 in Figure 3) remains bound to the metal. The overall geometry is a square pyramid (τ = 0.03) with the nitride in the apical position. The triflate anion is oriented toward a vacant site on Mo 2.65 Å away, which is long compared to a typical Mo−triflate bond (2.1−2.2 Å).[11]

The ^{1}H NMR spectrum (CD_2Cl_2, 25 °C) of **3** is consistent with its structure in the solid state. Distinctive features include doublets assigned to one set of benzyl proton resonances at 6.85 and 4.78 ppm (J = 20 Hz), similar to the benzyl proton resonances in **2a** and **2b**. Protons in the other benzyl position are coupled to the amine proton and are found as two doublet of doublet resonances at 5.29 and 4.59 ppm ($^2J_{HH}$ = 16 Hz; $^3J_{HH}$ = 4 Hz). The aniline proton resonance is a broad doublet at 6.90 ppm. Its identity was confirmed through TOSY (2D ^{1}H NMR) spectroscopy (see the SI).

Compounds That Contain Hydrogen Bonds. Compound **1** reacts with $[LutH][BAr^F{}_4]$ (Lut = 2,6-dimethylpyridine; $BAr^F{}_4^-$ = $\{B(3,5\text{-}(CF_3)_2C_6H_3)_4\}^-$) to generate $\{[Ar_2N_3]Mo(N)(O\text{-}t\text{-}Bu)(HLut)\}\{BAr^F{}_4\}$ (**4a**), in which the lutidinium cation is hydrogen-bonded to the nitride ligand (eq 3).

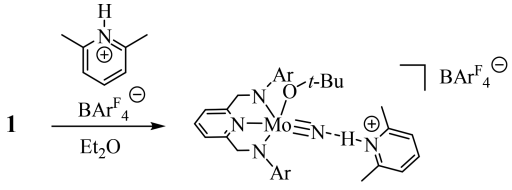

(3)

An X-ray study of **4a** (Figure 4) shows it to be approximately a square pyramid with the *tert*-butoxide ligand in the apical position [Mo−O = 1.8664(9) Å]. The Mo−N_{amide} bond distances are 1.9977(9) and 2.0223(9) Å, as found in compound **1** and in $[Ar_2N_3]Mo(N)(Cl)$.[8] The distance between N4 and H5A is 1.79(1) Å. An N4−N5 distance of 2.700(1) Å is a typical distance in a "weak" N···HN hydrogen bond.[12a]

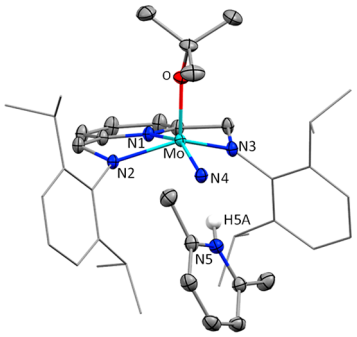

Figure 4. Molecular structure of **4a**. Ellipsoids are shown at 50% probability. The aryl groups are shown as wireframes, and one cocrystallized ether molecule, most hydrogen atoms, and the $BAr^F{}_4$ anion are omitted for clarity. Mo−N1 = 2.2424(9) Å, Mo−N2 = 2.0223(9) Å, Mo−N3 = 1.9977(9) Å, Mo−N4 = 1.6811(10) Å, Mo−O = 1.8664(9) Å, N4−N5 = 2.700(1) Å, N4···H5A = 0.1.79(1) Å, N2−Mo−N3 = 135.00(4)°, N4−Mo−O = 147.65(4)°, and τ = 0.21.

In $[LutH][BAr^F{}_4]$, the N−H stretch is observed at 3370 cm^{-1} in the solid-state IR spectrum (attenuated total reflectance, ATR). In **4a**, the N−H stretch is observed at 2959 cm^{-1} ($\Delta\nu$ = 411 cm^{-1}), which is in good agreement with an expected $\Delta\nu$ of 397 cm^{-1} given by the formula[12b] $\Delta\nu = 0.011 d_{HA}^{-6.1}$, where d_{HA} is the distance (in nanometers) between the proton and the acceptor atom in the X-ray study of **4a**.

Diagnostic features of the ^{1}H NMR spectrum of **4a** in CD_2Cl_2 (Figure 5) include a characteristic pair of benzyl

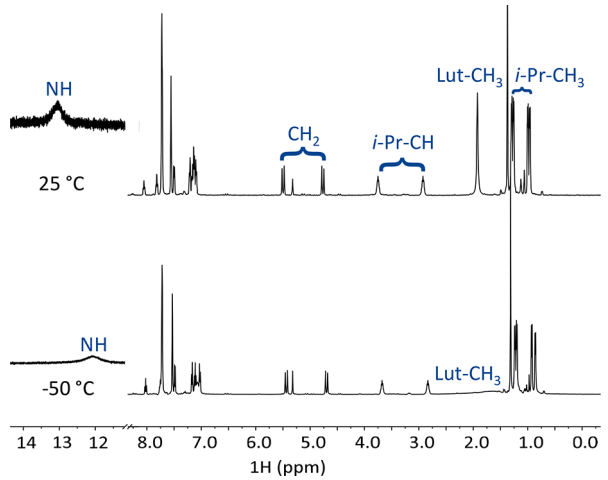

Figure 5. Variable-temperature NMR spectra of **4a** (CD_2Cl_2, 500 MHz). The Lut N−*H* resonances are shown at 25× intensity.

proton doublets at 5.48 and 4.75 ppm (J = 20 Hz) for a molecule of this type with mirror symmetry, two isopropyl methine septet resonances at 3.73 and 2.91 ppm, and four (overlapping) isopropyl methyl resonances. The aryl region shows two triplets that are assigned to the pyridine backbone of the bis(amido)pyridine ligand and the lutidinium ligand. A broad resonance is found at 13.14 ppm for the NH proton (Figure 5, top) versus 12.4 ppm in the NMR spectrum of

DOI: 10.1021/acs.inorgchem.8b03346
Inorg. Chem. 2019, 58, 3724−3731

[LutH][BAr^F_4] itself. A single sharp resonance at 1.94 ppm is assigned to the lutinidium methyl groups. At −50 °C, this methyl resonance broadens and almost disappears into the baseline (Figure 5, bottom). We propose that lutidinium is still dissociating and exchanging rapidly on the NMR time scale at −50 °C and is the main reason why the lutinidium methyl resonance is so broad. Alternatively, if lutidinium instead is essentially bound to the nitride at −50 °C, then the methyl groups in the 2 and 6 positions in $[LutH]^+$ could be becoming inequivalent as a consequence of a slowing of the rotation of $[LutH]^+$ in the sterically crowded "slot" between the two aryl groups.

UV/vis spectra of **1** in dichloromethane in the range of 300−450 nm at several concentrations of [LutH][BAr^F_4] are shown in Figure 6. These spectra are consistent with a

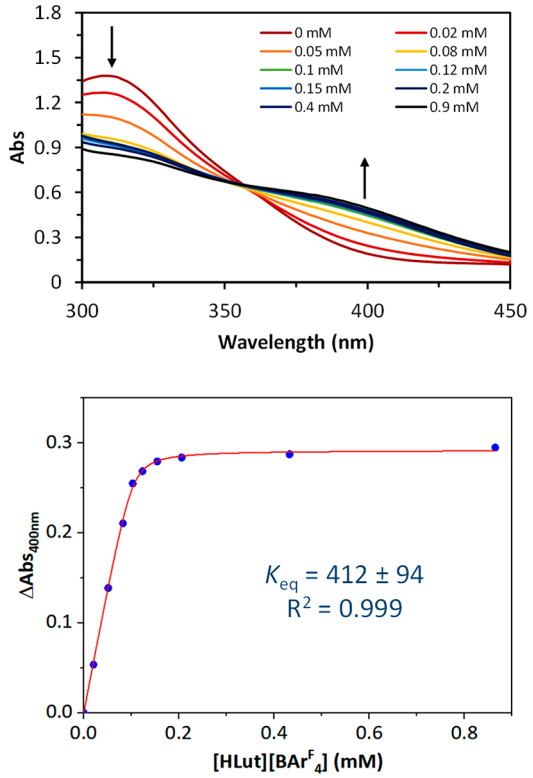

Figure 6. (Top) UV/vis spectra for **1** (0.1 mM in CH_2Cl_2) upon the successive addition of [LutH][BAr^F_4] (0−0.9 mM). (Bottom) Determination of K_{eq} for the equilibrium between **4a**, [LutH][BAr^F_4], and **1**.

decreasing amount of **1** (0.1 mM) and an increasing amount of **4a** as the concentration of [LutH][BAr^F_4] is increased from 0 to 0.9 mM. The presence of only **1** and **4a** is confirmed by an isosbestic point at 360 nm. A plot of [LutH][BAr^F_4] concentration versus change in absorbance (ΔAbs) at 400 nm (Figure 6 bottom) can be fit and K_{eq} extracted through a fitting model to give K_{eq} = 412 ± 94 (R^2 = 0.999; Figure 6, bottom).[13] This equilibrium constant corresponds to ΔG = −3.6 ± 0.8 kcal, a value that is consistent with a weak hydrogen bond.[12] At a total concentration of ∼0.1 M **4a**, the concentration of **1** and anilinium at 22 °C is ∼0.01 M (∼10% dissociated).

The addition of [2picH][BAr^F_4] ($[2picH]^+$ = 2-methylpyridinium) to **1** leads primarily to the formation of {[Ar_2N_3]Mo(N)(O-*t*-Bu)(H-2pic)}{BAr^F_4} (**4b**), a hydrogen-bonded derivative analogous to **4a**, according to ^{1}H NMR spectra. However, the reaction is complicated by the formation of one or more complexes in which the $[Ar_2N_3]^{2-}$ ligand is protonated, as described in the previous section. Pale-yellow **4b** can be isolated from the mixture in 70% yield. An ATR-IR spectrum of the isolated compound shows the picolinium N−H stretch redshift from 3375 cm^{-1} in free [2picH][BAr^F_4] to 2970 cm^{-1} in **4b**, a $\Delta\nu$ value (405 cm^{-1}) similar to the shift found in **4a**. The ^{1}H NMR spectrum of **4b** shows methylene doublet resonances at 5.49 and 4.87 ppm (J = 20 Hz), and the picolinium proton is a broad singlet at 11.3 ppm (see the SI for NMR details). Complex **4b** can be crystallized; however, with time its ^{1}H NMR spectrum degrades as it slowly decomposes to a significant degree over a period of 12 h at 22 °C to give one or more compounds in which the pincer ligand has been protonated at the amido nitrogen. We propose that when the $[Ar_2N_3]^{2-}$ ligand is protonated by the free $[2picH]^+$, 2-methylpyridine that is formed can then bind to the metal to yield at least one new adduct. In contrast, $[LutH]^+$ is too sterically hindered to deliver a proton to the amido nitrogen. Therefore, in an experiment analogous to that shown in Figure 6 using **4b** instead of **4a**, a well-defined isosbestic point is not observed and K_{eq} in **4b** cannot be determined accurately. However, the red shift in the IR spectrum of **4b** suggests that the hydrogen bond that is formed between **1** and $[2picH]^+$ is similar in strength to that formed between **1** and $[LutH]^+$. It should be noted that the pK_a difference between picolinium (5.96 in water) and 2,6-lutidinium (6.72),[14] is small. It is simply the smaller *size* of $[2picH]^+$ that allows protonation of the $[Ar_2N_3]^{2-}$ ligand to compete with formation of a hydrogen bond to the nitride.

When [pyH][BAr^F_4] ($[pyH]^+$ = pyridinium) is added to **1** in dichloromethane, ^{1}H NMR spectra suggest that a relatively complex mixture is formed, with one or more pincer-protonated complexes being formed (Figure S23). In this case, the conjugate base (pyridine) is certainly likely to bind to a cationic metal center. and isomers of a monopyridine adduct are further possible complications.

Reductions by Cobaltocene. Some form of proton-coupled electron transfer (PCET)[15] has been proposed to assist addition of the first proton and electron to (HIPTN$_3$N)Mo(N$_2$) to yield (HIPTN$_3$N)Mo(N═NH)[1] (HIPT = [{3,5-(2,4,6-*i*-$Pr_3C_6H_2$)$_2$C$_6$H$_3$NCH$_2$CH$_2$}$_3$N]$^{3-}$) and to be involved at some other stage in a variety of other homogeneous reductions of dinitrogen by molybdenum, iron, or other catalysts. Although it is not obvious why PCET would be required to add a proton and electron to a nitride, an interesting fundamental question is whether **4a** would be reduced by cobaltocene to yield "[Ar_2N_3]Mo(NH)(O-*t*-Bu)". In order for this to be the case, electron transfer from $CoCp_2$ to **4a** must be much faster than any electron transfer from $CoCp_2$ to "free" lutidinium. If [Ar_2N_3]Mo(NH)(O-*t*-Bu) can be formed from **4a**, there is no guarantee that it will be stable toward the formation of hydrogen and **1**.

Cobaltocene reacts immediately with **4a** in C_6D_6 at 22 °C to give **1** (Scheme 2). At −78 °C in diethyl ether, the components form a solution when mixed whose color is similar to ether solutions of **1**. Compound **3** also reacts with cobaltocene to yield **1**. We assume that H_2 is formed in each case.

DOI: 10.1021/acs.inorgchem.8b03346
Inorg. Chem. 2019, 58, 3724−3731

Scheme 2

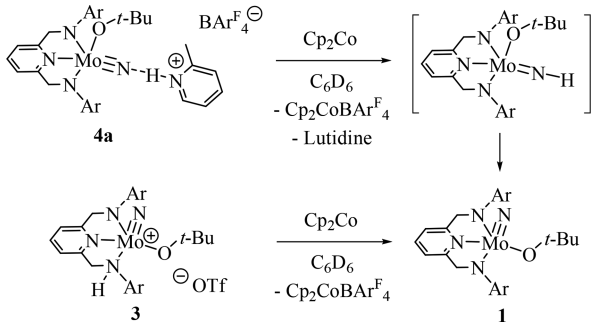

DISCUSSION

We have explored the "simple" addition of a proton to a nitride complex that has been shown to be a catalyst or catalyst precursor for the reduction of molecular nitrogen to ammonia in diethyl ether between −78 and +22 °C in a batchwise manner with $CoCp^*_2$ as the electron source and $[Ph_2NH_2][OTf]$ as the proton source. Protonation of a nitride is only one step in a complex mechanism that involves the addition of six protons and six electrons to molecular nitrogen to produce ammonia, with hydrogen being an alternative product. We were not especially surprised to find that an amido nitrogen in the $[2,6\text{-}(ArNCH_2)_2NC_5H_3]^{2-}$ ligand appears to be the kinetic site for protonation. However, we were surprised to find that (i) *tert*-butoxide is not protonated in **1** by an acid relevant to nitrogen reduction ($[Ph_2NH_2][OTf]$) and (ii) a sterically demanding acid (lutidinium in $[LutH][BAr^F_4]$) hydrogen-bonds to the nitride, but the proton is *not* delivered to give the Mo═NH cationic complex.

We have not been able to find another example of hydrogen bonding of a protonic acid to a metal nitride in the literature. The donor−acceptor bond distance and NH stretching frequencies measured in the solid state are in agreement with a hydrogen bond. Furthermore, the hydrogen bond is maintained in dichloromethane, as evidenced by ^{1}H NMR and UV/vis spectroscopies. The characterization of **4a** demonstrates that hydrogen-bonded intermediates may be relevant in understanding the PCET reactions relevant to nitrogen reduction. In principal, a hydrogen-bonded adduct could be a precursor to a PCET reaction by bringing the proton within the necessary distance to the nitride, and the addition of an electron source facilitates the transfer.[16] However, a weak hydrogen bond allows the acid to dissociate; ∼10% at 22 °C was observed here. The relative rates of delivering an electron to the hydrogen-bonded complex versus free acid in equilibrium with it becomes a key issue if the acid is not completely bound.

It is clear that hydrogen bonding to the nitride in **1** by lutidinium in $[LutH][BAr^F_4]$ is favored over protonation to give $\{[Ar_2N_3]Mo(NH)(O\text{-}t\text{-}Bu)\}BAr^F_4$ and that a sterically less demanding and stronger acid protonates the amido nitrogen in the $[Ar_2N_3]^{2-}$ ligand. However, *tert*-butoxide can be protonated and replaced if X^- (e.g., Cl^- or RO^-) in HX can bind to the metal, even when the pK_a value of HX is high (e.g., for ROH).[8] This concept is illustrated by two additional examples: [LutH][Cl] reacts with **1** to give $[Ar_2N_3]Mo(N)Cl$,[8] and [LutH][OTf] reacts with **1** to give **3** in ether (Figure S28).

CONCLUSIONS

In this report, we have demonstrated that the product of adding acid to **1** depends dramatically on the acid and anion of that acid. Full protonolysis, pincer ligand protonation, and hydrogen bonding have all been observed with complex **1**, depending on the characteristics of the proton source, but the protonation of neither *tert*-butoxide nor nitride (with a catalytically relevant acid) is observed. Interestingly, the results here are guided by *steric factors* of the acids, not only pK_a values. While we are a long way from our goal of understanding how catalytic dinitrogen reduction with **1** is accomplished, we have shown that the protonation of nitride cannot be taken for granted and that hydrogen bonding even to a nitride must be considered among the plausible phenomena in a catalytic cycle for dinitrogen reduction by **1**.

EXPERIMENTAL SECTION

All air- and moisture-sensitive materials were manipulated under a nitrogen atmosphere in a Vacuum Atmospheres glovebox or on a dual-manifold Schlenk line. All glassware was oven- or flame-dried prior to use. Benzene, tetrahydrofuran (THF), diethyl ether, *n*-hexane, and toluene were degassed, passed through activated alumina columns, and stored over 4 Å Linde-type molecular sieves prior to use. Pentane was washed with H_2SO_4, followed by water and saturated aqueous $NaHCO_3$, and dried over $CaCl_2$ pellets for at least 2 weeks prior to use in the solvent purification system. Deuterated solvents were dried over 4 Å Linde-type molecular sieves prior to use. $[2,6\text{-}(ArNHCH_2)_2NC_5H_3]$ (Ar = 2,6-diisopropylphenyl),[17] $\{Ph_2NH_2\}\{OTf\}$,[3b] **1**,[8] and $[Ar_2N_3]Mo(N)Cl$[8] were prepared according to literature procedures. NMR spectra were measured on Varian spectrometers. Chemical shifts for ^{1}H and ^{13}C NMR spectra are reported as parts per million relative to tetramethylsilane and referenced to the residual ^{1}H or ^{13}C resonances of the deuterated solvent (^{1}H, benzene δ 7.16, methylene chloride δ 5.32; ^{13}C, benzene δ 128.06, methylene chloride δ 53.84). ^{19}F{^{1}H} NMR (470 MHz) spectra were recorded in a proton-decoupled mode and referenced to external standard $CFCl_3$. Fourier transform infared spectra were recorded on a Bruker Alpha II equipped with a Platinum ATR single reflection diamond ATR module. UV/vis spectra were measured on an Agilent 8453 UV/vis spectroscopy system. Elemental analysis was conducted by Atlantic Microlab, Inc.

$[HAr_2N_3]Mo(N)(OAd)_2$ (2a). Compound **1** (52 mg, 0.081 mmol) and HOAd (25 mg, 0.163 mmol) were dissolved in CD_2Cl_2 and heated at 90 °C for 2 h. After conversion was observed by ^{1}H NMR, the solvents were removed in vacuo, giving **2a** as an off-white powder (56 mg, 96% yield). ^{1}H NMR (CD_2Cl_2, 300 MHz): δ 7.60 (t, J = 8 Hz, 1H, py−*H*), 7.25 (mult, 4H, Ar−*H*), 7.00 (mult, 4H, Ar−*H*), 4.77 (s, 2H, C*H*$_2$), 4.50 (dd, J = 20 Hz, J = 8 Hz, 2H, C*H*$_2$), 4.06 (t, J = 8 Hz, N*H*), 3.42 (sept, J = 7 Hz, 2H, *i*-Pr−C*H*), 3.19 (sept, J = 7 Hz, 2H, *i*-Pr−C*H*), 2.13 (s, 3H, Ad−*H*), 1.80 (mult, 6H, Ad−*H*), 1.70 (s, 6H, Ad−*H*), 1.60 (s, 6H, Ad−*H*), 1.45 (s, 18H, *t*-Bu), 1.34 (d, J = 7 Hz, 6H, *i*-Pr−C*H*$_3$), 1.22 (d, J = 7 Hz, 6H, *i*-Pr−C*H*$_3$), 1.09 (d, J = 7 Hz, 12H, *i*-Pr−C*H*$_3$), 0.88 (t, J = 7 Hz, 3H, Ad−*H*). ^{13}C{^{1}H} NMR (100 MHz, CD_2Cl_2, 25 °C): δ 161.0, 159.2, 158.3, 143.4, 143.0, 142.9, 137.7, 126.1, 124.4, 124.0, 123.7, 121.3, 118.8, 77.9, 67.2, 55.4, 46.0, 45.8, 36.7, 36.5, 31.9, 31.3, 28.0, 27.7, 26.3, 25.4, 24.5, 22.8. Several attempted elemental analyses of **2a** were not consistent and failed, although **2b** (below) did analyze readily. The cause of the problem with **2a** has not been determined.

$[HAr_2N_3]Mo(N)(O\text{-}t\text{-}Bu)_2$ (2b). 2,6-$[ArHNCH_2]_2NC_5H_3$ (100 mg, 0.22 mmol) was dissolved in diethyl ether (5 mL), and the solution was chilled to −35 °C. Li-*n*-Bu (136 μL, 1.6 M in hexane, 0.22 mmol) was added in one portion, while the reaction mixture was kept cold. The solution turned yellow, and $Mo(N)(O\text{-}t\text{-}Bu)_3$ (72 mg, 0.22 mmol) was added as a solid. The resulting solution was stirred for 1 h to give a pale-purple solution. The volatiles were removed in vacuo, the dry solid was dissolved in pentane (∼2 mL), and

DOI: 10.1021/acs.inorgchem.8b03346
Inorg. Chem. 2019, 58, 3724−3731

crystallization was carried out at −35 °C. The mother liquor was decanted, and the crystals were exposed to vacuum to give **2b** (90 mg, 58% yield). ^{1}H NMR (CD_2Cl_2, 500 MHz): δ 7.60 (t, J = 8 Hz, 1H, py−H), 7.22 (s, 2H, Ar−H), 7.16 (d, J = 8 Hz, 1H, py−H), 7.03 (s, 2H, Ar−H), 4.77 (s, 2H, CH_2), 4.48 (d, J = 8 Hz, 2H, CH_2), 4.06 (t, J = 8 Hz, 1H, NH), 3.43 (sept, J = 7 Hz, 2H, i-Pr−CH), 3.20 (sept, J = 8 Hz, 2H, i-Pr−CH), 1.45 (s, 18H, t-Bu), 1.34 (d, J = 7 Hz, 6H, i-Pr−CH_3), 1.22 (d, J = 7 Hz, 6H, i-Pr−CH_3), 1.09 (d, J = 7 Hz, 12H, i-Pr−CH_3). ^{13}C{^{1}H} NMR (100 MHz, CD_2Cl_2, 25 °C): δ 160.8, 159.2, 158.4, 143.3, 142.8, 137.7, 126.1, 124.4, 124.0, 123.8, 121.4, 119.0, 79.2, 67.3, 55.4, 35.5, 31.8, 27.9, 27.7, 26.2, 25.4, 24.5. Anal. Calcd for $C_{39}H_{60}MoN_4O_2$: C, 65.71; H, 8.48; N, 7.86. Found: C, 65.63; H, 8.51; N, 7.81.

{[HAr$_2$N$_3$]Mo(N)(O-*t*-Bu)}{OTf} (3). Compound **1** (90 mg, 0.14 mmol) was dissolved in diethyl ether. $[H_2NPh_2][OTf]$ (45 mg, 0.14 mmol) was added as a solid over the course of 1 min. The mixture was stirred until a yellow precipitate was observed. The precipitate was recovered on a filter, giving **3** as an orange powder (67 mg, 60% yield). Crystals suitable for X-ray diffraction were grown from a saturated THF solution layered with pentane and left overnight at room temperature. ^{1}H NMR (CD_2Cl_2, 500 MHz): δ 8.11 (t, J = 8 Hz, 1H, py−H), 7.52 (d, J = 8 Hz, 1H, py−H), 7.47 (d, J = 8 Hz, 1H, py−H), 7.29 (d, J = 8 Hz, 1H, Ar−H), 7.26 (d, J = 8 Hz, 2H, Ar−H), 7.20 (d, J = 8 Hz, 2H, Ar−H), 7.09 (d, J = 8 Hz, 1H, Ar−H), 6.90 (broad d, J = 10 Hz, 1H, NH), 6.85 (d, J = 20 Hz, 1H, CH_2), 5.29 (dd, J = 16.2 Hz, J = 4 Hz, 1H, CH_2), 4.78 (d, J = 20 Hz, 1H, CH_2), 4.59 (dd, J = 16.2 Hz, J = 4 Hz, 1H, CH_2), 3.92 (sept, J = 7 Hz, 1H, i-Pr−CH, 3.55 (sept, J = 7 Hz, 1H, i-Pr−CH), 3.41 (sept, J = 7 Hz, 1H, i-Pr−CH), 3.14 (sept, J = 7 Hz, 1H, i-Pr−CH), 1.37 (d, J = 7 Hz, 3H, i-Pr−CH_3), 1.26 (d, J = 7 Hz, 3H, i-Pr−CH_3), 1.24 (d, J = 7 Hz, 3H, i-Pr−CH_3), 1.17 (d, J = 7 Hz, 3H, i-Pr−CH_3), 1.14 (d, J = 7 Hz, 3H, i-Pr−CH_3), 1.10 (d, J = 7 Hz, 3H, i-Pr−CH_3), 1.07 (d, J = 7 Hz, 3H, i-Pr−CH_3), 1.02 (d, J = 7 Hz, 3H, i-Pr−CH_3), 1.00 (s, 9H, t-Bu). ^{13}C{^{1}H} NMR (CD_2Cl_2, 125 MHz, 25 °C): δ 170.2, 158.5, 155.0, 144.4, 143.2, 143.1, 142.1, 141.1, 139.0, 129.2, 128.0, 127.0, 126.9, 125.7, 124.3, 122.4, 120.7, 119.5, 117.5, 110.0, 82.2, 71.1, 61.1, 30.3, 28.8, 28.3, 27.6, 27.3, 26.7, 25.3, 25.0, 23.4, 23.0, 22.2, 22.1. ^{19}F{^{1}H} NMR (CD_2Cl_2, 470 MHz, 25 °C): δ −77.3. Anal. Calcd for $C_{38}H_{53}F_3MoN_4O_4SCl_2$ (**3**·CH_2Cl_2): C, 50.86; H, 6.11; N, 6.41. Found: C, 51.15; H, 6.19; N, 6.40. One molecule of CH_2Cl_2 is present in crystals grown from CH_2Cl_2/pentane for microanalysis and observed by ^{1}H NMR spectroscopy in CD_3CN.

{[Ar$_2$N$_3$]Mo(N)(O-*t*-Bu)(HLut)}{BAr$^F_4$} (4a). Compound **1** (77 mg, 0.12 mmol) was stirred in CH_2Cl_2 (2 mL), and [LutH][BAr$^F_4$] (117 mg, 0.12 mmol) was added as a solid over the course of 1 min. The yellow solution was stirred for 10 min, then layered with pentane, and stored at −35 °C until pale crystals formed. The mother liquor was decanted and the remaining off-white material dried under vacuum, giving **4a** (148 mg, 76% yield). Crystals suitable for X-ray diffraction were grown from an ether solution of **4a** layered with pentane and stored at −35 °C overnight. ^{1}H NMR (CD_2Cl_2, 500 MHz): δ 13.07 (broad s, 1H, Lut−NH), 8.04 (t, J = 8 Hz, 1H, py−H), 7.81 (t, J = 8 Hz, 1H, Lut−H), 7.71 (s, 8H, BAr$^F_4$ o-H), 7.54 (s, 4H, BAr$^F_4$ p-H), 7.50 (d, J = 8 Hz, 2H, py−H), 7.18 (mult, 6H, Ar−H), 5.48 (d, J = 20 Hz, 2H, CH_2), 4.75 (d, J = 20 Hz, 2H, CH_2), 3.73 (sept, J = 7 Hz, 2H, i-Pr−CH), 2.91 (sept, J = 7 Hz, 2H, i-Pr−CH), 1.94 (s, 6H, Lut−CH_3), 1.36 (s, 9H, t-Bu), 1.28 (d, J = 7 Hz, 6H, i-Pr−CH_3), 1.24 (d, J = 7 Hz, 6H, i-Pr−CH_3), 0.98 (d, J = 7 Hz, 6H, i-Pr−CH_3), 0.94 (d, J = 7 Hz, 6H, i-Pr−CH_3). ^{13}C{^{1}H} NMR (125 MHz, CD_2Cl_2, 25 °C): δ 162.3, 159.1, 154.9, 144.1, 142.8, 141.0, 135.2, 129.4, 126.7, 126.1, 124.9, 124.3, 123.9, 118.6, 117.9, 110.4, 82.0, 70.3, 32.3, 28.6, 27.6, 26.2, 25.2, 24.7, 19.6. ^{19}F{^{1}H} NMR (CD_2Cl_2, 470 MHz, 25 °C): δ −62.9. Anal. Calcd for $C_{74}H_{72}BF_{24}MoN_5O$: C, 55.20; H, 4.51; N, 4.35. Found: C, 54.74; H, 4.37; N, 4.26.

{[Ar$_2$N$_3$]Mo(N)(O-*t*-Bu)(H-2pic)}{BAr$^F_4$} (4b). Compound **1** (50 mg, 0.08 mmol) was stirred in CH_2Cl_2 (2 mL), and [2picH][BAr$^F_4$] (75 mg, 0.08 mmol) was added slowly as a solid. The yellow solution was stirred for 10 min, layered with pentane, and stored at −35 °C until pale crystals formed. The mother liquor was decanted and the remaining off-white material dried under vacuum, giving **4b** (90 mg, 70% yield). ^{1}H NMR (CD_2Cl_2, 500 MHz): δ 13.04 (broad s, 1H, 2pic−NH), 8.10 (t, J = 8 Hz, 1H, py−H), 7.87 (t, J = 8 Hz, 1H, 2pic−H), 7.72 (s, 8H, BAr$^F_4$ o-H), 7.55 (s, 4H, BAr$^F_4$ p-H), 7.25 (mult, 10H, Ar−H), 5.52 (d, J = 20 Hz, 2H, CH_2), 4.87 (d, J = 20 Hz, 2H, CH_2), 3.85 (sept, J = 7 Hz, 2H, i-Pr−CH), 2.65 (sept, J = 7 Hz, 2H, i-Pr−CH), 1.83 (s, 3H, 2pic−CH_3), 1.38 (d, J = 7 Hz, 6H, i-Pr−CH_3), 1.31 (s, 9H, t-Bu), 1.27 (d, J = 7 Hz, 6H, i-Pr−CH_3), 1.10 (d, J = 7 Hz, 6H, i-Pr−CH_3), 0.86 (d, J = 7 Hz, 6H, i-Pr−CH_3). ^{13}C{^{1}H} NMR (100 MHz, CD_2Cl_2): δ 163.0, 162.5, 162.0, 161.5, 159.5, 159.0, 145.3, 144.0, 142.7, 141.9, 141.5, 135.3, 129.5, 129.2, 127.2, 126.8, 126.8, 126.4, 124.9, 124.8, 123.8, 123.7, 119.1, 118.0, 70.1, 32.7, 31.6, 30.7, 28.6, 27.8, 26.05, 25.1, 24.6. Multiple attempts to analyze **4b** have failed.

UV/Vis Studies. A total of 1.5 mL of a 0.2 mM stock solution of **1** in CH_2Cl_2 was added to a cuvette. A volume of a 1 mM stock solution of [HLut][BAr$^F_4$] in CH_2Cl_2 was added based on the desired equivalents. The total volume was brought to 3 mL in the cuvette using CH_2Cl_2. Measurements were recorded within the time of mixing and delivering of the cuvette to the spectrometer. The plot of [HLut$^+$] concentration versus ΔAbs was fit to a binding equation with refinement of [**1**], K_{eq}, and a scaling factor. See the SI for full details.

Electron Paramagnetic Resonance (EPR) Studies. In response to a reviewer's comment concerning the possibility of paramagnetic impurities in samples that failed elemental analyses, several reactions were explored through EPR studies of the reaction mixtures. **1** (3 mg, 0.005 mmol) was dissolved in 10 mL of 2-methyltetrahydrofuran (460 μM solution). The acid (1.5 mg of $[Ph_2NH_2][OTf]$, 1.5 mg of HOAd, 4.5 mg of ([HLut][BAr$^F_4$], and 4.5 mg of [H-2pic][BAr$^F_4$]) was added to the solution, and an aliquot (0.4 mL) of the total solution was transferred to an EPR tube. X-band EPR measurements (9.3684 GHz, 0.6325 mW power, 25 dB attenuation) were conducted at 10 K. Virtually no signals were found that could be ascribed to molybdenum(V). The reactions examined include **1** + $[Ph_2NH_2]$-[OTf], **1** + 2HOAd, **1** + [HLut][BAr$^F_4$], and **1** + [H-2pic][BAr$^F_4$].

■ ASSOCIATED CONTENT

Supporting Information

The Supporting Information is available free of charge on the ACS Publications website at DOI: 10.1021/acs.inorgchem.8b03346.

NMR and spectral data for all compounds and X-ray crystallographic files for the reported structures (PDF)

Accession Codes

CCDC 1872128−1872131 contain the supplementary crystallographic data for this paper. These data can be obtained free of charge via www.ccdc.cam.ac.uk/data_request/cif, or by emailing data_request@ccdc.cam.ac.uk, or by contacting The Cambridge Crystallographic Data Centre, 12 Union Road, Cambridge CB2 1EZ, UK; fax: +44 1223 336033.

■ AUTHOR INFORMATION

Corresponding Author

*E-mail: rrs@mit.edu.

ORCID

Richard R. Schrock: 0000-0001-5827-3552

Notes

The authors declare no competing financial interest.

■ ACKNOWLEDGMENTS

We are grateful for financial support from the Department of Energy (Grant DE-SC0013307). We also thank the NSF for support of X-ray diffraction instrumentation (Grant CHE-0946721).

DOI: 10.1021/acs.inorgchem.8b03346
Inorg. Chem. 2019, 58, 3724−3731

REFERENCES

(1) (a) Yandulov, D. V.; Schrock, R. R. Catalytic Reduction of Dinitrogen to Ammonia at a Single Molybdenum Center. *Science* **2003**, *301*, 76−78. (b) Hetterscheid, D. G. H.; Hanna, B. S.; Schrock, R. R. Molybdenum Triamidoamine Systems. Reactions Involving Dihydrogen Relevant to Catalytic Reduction of Dinitrogen. *Inorg. Chem.* **2009**, *48*, 8569−8577. (c) Schrock, R. R. Catalytic Reduction of Dinitrogen to Ammonia by Molybdenum. In *Catalysis without Precious Metals*; Bullock, R. M., Ed.; Wiley-VCH, 2010; p 25. (d) Munisamy, T.; Schrock, R. R. An Electrochemical Investigation of Intermediates and Processes Involved in the Catalytic Reduction of Dinitrogen by [HIPTN$_3$N]Mo (HIPTN$_3$N = (3,5-(2,4,6-*i*-Pr$_3$C$_6$H$_2$)$_2$C$_6$H$_3$NCH$_2$CH$_2$)$_3$N). *Dalton Trans.* **2012**, *41*, 130−137. (e) Schrock, R. R. Catalytic Reduction of Dinitrogen to Ammonia at a Single Molybdenum Center. *Acc. Chem. Res.* **2005**, *38*, 955−962. (f) Yandulov, D.; Schrock, R. R. Reduction of Dinitrogen to Ammonia at a Well-Protected Reaction Site in a Molybdenum Triamidoamine Complex. *J. Am. Chem. Soc.* **2002**, *124*, 6252−6253. (g) van der Ham, C. J. M.; Koper, M. T. M.; Hetterscheid, D. G. H. Challenges in Reduction of Dinitrogen by Proton and Electron Transfer. *Chem. Soc. Rev.* **2014**, *43*, 5183−5191. (h) Schrock, R. R. Catalytic Reduction of Dinitrogen to Ammonia by Molybdenum. Theory Versus Experiment. *Angew. Chem., Int. Ed.* **2008**, *47*, 5512−5522.

(2) (a) Arashiba, K.; Miyake, Y.; Nishibayashi, Y. A molybdenum complex bearing PNP-type pincer ligands leads to the catalytic reduction of dinitrogen into ammonia. *Nat. Chem.* **2011**, *3*, 120−125. (b) Nishibayashi, Y. Molybdenum-Catalyzed Reduction of Molecular Dinitrogen Under Mild Reaction Conditions. *Dalton Trans.* **2012**, *41*, 7447−7453. (c) Kinoshita, E.; Arashiba, K.; Kuriyama, S.; Eizawa, A.; Nakajima, K.; Nishibayashi, Y. Synthesis and Catalytic Activity of Molybdenum-Nitride Complexes Bearing Pincer Ligands. *Eur. J. Inorg. Chem.* **2015**, *2015*, 1789−1794. (d) Arashiba, K.; Kinoshita, E.; Kuriyama, S.; Eizawa, A.; Nakajima, K.; Tanaka, H.; Yoshizawa, K.; Nishibayashi, Y. Catalytic Reduction of Dinitrogen to Ammonia by Use of Molybdenum-Nitride Complexes Bearing a Tridentate Triphosphine as Catalysts. *J. Am. Chem. Soc.* **2015**, *137*, 5666−5669. (e) Tanaka, H.; Nishibayashi, Y.; Yoshizawa, K. Interplay between Theory and Experiment for Ammonia Synthesis Catalyzed by Transition Metal Complexes. *Acc. Chem. Res.* **2016**, *49*, 987−995. (f) Tanabe, Y.; Nishibayashi, Y. Catalytic Dinitrogen Fixation to Form Ammonia at Ambient Reaction Conditions Using Transition Metal-Dinitrogen Complexes. *Chem. Rec.* **2016**, *16*, 1549−1577. (g) Kinoshita, E.; Arashiba, K.; Kuriyama, S.; Miyake, Y.; Shimazaki, R.; Nakanishi, H.; Nishibayashi, Y. Synthesis and Catalytic Activity of Molybdenum-Dinitrogen Complexes Bearing Unsymmetric PNP-Type Pincer Ligands. *Organometallics* **2012**, *31*, 8437−8443. (h) Nishibayashi, Y. Recent Progress in Transition-Metal-Catalyzed Reduction of Molecular Dinitrogen under Ambient Reaction Conditions. *Inorg. Chem.* **2015**, *54*, 9234−9247.

(3) (a) Anderson, J. S.; Rittle, J.; Peters, J. C. Catalytic Conversion of Nitrogen to Ammonia by an Iron Model Complex. *Nature* **2013**, *501*, 84−87. (b) Chalkley, M. J.; Del Castillo, T. J.; Matson, B. D.; Roddy, J. P.; Peters, J. C. Catalytic N_2-to-NH_3 Conversion by Fe at Lower Driving Force: A Proposed Role for Metallocene-Mediated PCET. *ACS Cent. Sci.* **2017**, *3*, 217−223.

(4) Fajardo, Jr. J. F.; Peters, J. C. Catalytic Nitrogen-to-Ammonia Conversion by Osmium and Ruthenium Complexes. *J. Am. Chem. Soc.* **2017**, *139*, 16105−16108.

(5) (a) Arashiba, K.; Eizawa, A.; Tanaka, H.; Nakajima, K.; Yoshizawa, K.; Nishibayashi, Y. Catalytic Nitrogen Fixation via Direct Cleavage of NitrogenNitrogen Triple Bond of Molecular Dinitrogen under Ambient Reaction Conditions. *Bull. Chem. Soc. Jpn.* **2017**, *90*, 1111−1118. (b) Laplaza, C. E.; Cummins, C. C. Dinitrogen Cleavage by a Three-Coordinate Molybdenum(III) Complex. *Science* **1995**, *268*, 861−863. (c) Laplaza, C. E.; Johnson, M. J. A.; Peters, J. C.; Odom, A. L.; Kim, E.; Cummins, C. C.; George, G. N.; Pickering, I. J. Dinitrogen Cleavage by Three-Coordinate Molybdenum(III) Complexes: Mechanistic and Structural Data. *J. Am. Chem. Soc.* **1996**, *118*, 8623−8638. (d) Solari, E.; DaSilva, C.; Iacono, B.; Hesschenbrouck, J.; Rizzoli, C.; Scopelliti, R.; Floriani, C. Photochemical Activation of the N≡N Bond in a Dimolybdenum-Dinitrogen Complex: Formation of a Molybdenum Nitride. *Angew. Chem., Int. Ed.* **2001**, *40*, 3907−3909. (e) Curley, J. J.; Cook, T. R.; Reece, S. Y.; Müller, P.; Cummins, C. C. Shining Light on Dinitrogen Cleavage: Structural Features, Redox Chemistry, and Photochemistry of the Key Intermediate Bridging Dinitrogen Complex. *J. Am. Chem. Soc.* **2008**, *130*, 9394−9405. (f) Huss, A. S.; Curley, J. J.; Cummins, C. C.; Blank, D. A. Relaxation and Dissociation Following Photoexcitation of the (μ-N$_2$)[Mo(N[t-Bu]Ar)$_3$]$_2$ Dinitrogen Cleavage Intermediate. *J. Phys. Chem. B* **2013**, *117*, 1429−1436. (g) Miyazaki, T.; Tanaka, H.; Tanabe, Y.; Yuki, M.; Nakajima, K.; Yoshizawa, K.; Nishibayashi, Y. Cleavage and Formation of Molecular Dinitrogen in a Single System Assisted by Molybdenum Complexes Bearing Ferrocenyldiphosphine. *Angew. Chem., Int. Ed.* **2014**, *53*, 11488−11492. (h) Silantyev, G. A.; Foerster, M.; Schluschass, B.; Abbenseth, J.; Wuertele, C.; Volkmann, C.; Holthausen, M. C.; Schneider, S. Dinitrogen Splitting Coupled to Protonation. *Angew. Chem., Int. Ed.* **2017**, *56*, 5872−5876. (i) Hebden, T. J.; Schrock, R. R.; Takase, M. K.; Müller, P. Cleavage of Dinitrogen to Yield a (*t*-BuPOCOP)Molybdenum(IV) Nitride. *Chem. Commun.* **2012**, *48*, 1851−1853.

(6) Chalkley, M. J.; Del Castillo, T. J.; Matson, B. D.; Peters, J. C. Fe-Mediated Nitrogen Fixation with a Metallocene Mediator: Exploring pK_a Effects and Demonstrating Electrocatalysis. *J. Am. Chem. Soc.* **2018**, *140*, 6122−6129.

(7) Chen, J. G.; Crooks, R. M.; Seefeldt, L. C.; Bren, K. L.; Bullock, R. M.; Darensbourg, M. Y.; Holland, P. L.; Hoffman, B.; Janik, M. J.; Jones, A. K.; Kanatzidis, M. G.; King, P.; Lancaster, K. Y.; Lymar, S. V.; Pfromm, P.; Schneider, W. F.; Schrock, R. R. Beyond Fossil-Fuel-Driven Nitrogen Transformations. *Science* **2018**, *360*, 873−890.

(8) Wickramasinghe, L. A.; Ogawa, T.; Schrock, R. R.; Müller, P. Reduction of Dinitrogen to Ammonia Catalyzed by Molybdenum Diamido Complexes. *J. Am. Chem. Soc.* **2017**, *139*, 9132−9135.

(9) Sinha, A.; Lopez, L. P. H.; Schrock, R. R.; Hock, A. S.; Mueller, P. Reactions of M(N-2,6-*i*-Pr$_2$C$_6$H$_3$)(CHR)(CH$_2$R‘)$_2$ (M = Mo, W) Complexes with Alcohols To Give Olefin Metathesis Catalysts of the Type M(N-2,6-*i*-Pr$_2$C$_6$H$_3$)(CHR)(CH$_2$R‘)(OR“). *Organometallics* **2006**, *25*, 1412−1423.

(10) Addison, A. W.; Rao, T. N.; Reedijk, J.; Van Rijn, J.; Verschoor, G. C. Synthesis, Structure, and Spectroscopic Properties of Copper(II) Compounds Containing Nitrogen-Sulfur Donor Ligands: the Crystal and Molecular Structure of Aqua[1,7-bis(N-Methylbenzimidazol-2’-yl)-2,6-dithiaheptane]Copper(II) Perchlorate. *J. Chem. Soc., Dalton Trans.* **1984**, 1349−1356.

(11) For recent examples, see: (a) Sues, P. E.; John, J. M.; Schrock, R. R.; Müller, P. Molybdenum and Tungsten Alkylidene and Metallacyclobutane Complexes That Contain a Dianionic Biphenolate Pincer Ligand. *Organometallics* **2016**, *35*, 758−761. (b) Yuki, M.; Miyake, Y.; Nishibayashi, Y.; Wakiji, I.; Hidai, M. Synthesis and Reactivity of Tungsten- and Molybdenum-Dinitrogen Complexes Bearing Ferrocenyldiphosphines Toward Protonolysis. *Organometallics* **2008**, *27*, 3947−3953. (c) Margulieux, G. W.; Bezdek, M. J.; Turner, Z. R.; Chirik, P. J. Ammonia Activation, H_2 Evolution and Nitride Formation from a Molybdenum Complex with a Chemically and Redox Noninnocent Ligand. *J. Am. Chem. Soc.* **2017**, *139*, 6110−6113.

(12) (a) Steiner, T. The Hydrogen Bond in the Solid State. *Angew. Chem., Int. Ed.* **2002**, *41*, 48−76. (b) Rozenberg, M.; Loewenschuss, A.; Marcus, Y. An Empirical Correlation Between Stretching Vibration Red-Shift and Hydrogen Bond Length. *Phys. Chem. Chem. Phys.* **2000**, *2*, 2699−2673.

(13) Chiang, K. P.; Barrett, P. M.; Ding, F.; Smith, J. M.; Kingsley, S.; Brennessel, W. W.; Clark, M. M.; Lachicotte, R. J.; Holland, P. L. Ligand Dependence of Binding to Three-Coordinate Fe(II) Complexes. *Inorg. Chem.* **2009**, *48*, 5106−5116.

(14) (a) Rochester, C. H. Acidity of Some Methyl-substituted Pyridinium Ions in Methanol. *J. Chem. Soc. B* **1967**, 33−36. (b) Andon, R. J. L.; Cox, J. D.; Herington, E. F. G. Ultraviolet

DOI: 10.1021/acs.inorgchem.8b03346
Inorg. Chem. 2019, 58, 3724−3731

Absorption Spectra and Dissociation Constants of Certain Pyridine Bases in Aqueous Solution. *Trans. Faraday Soc.* **1954**, *50*, 918−927.
(15) (a) Costentin, C. Electrochemical Approach to the Mechanistic Study of Proton-Coupled Electron Transfer. *Chem. Rev.* **2008**, *108*, 2145−2179. (b) Huynh, M. H. V.; Meyer, T. J. Proton-Coupled Electron Transfer. *Chem. Rev.* **2007**, *107*, 5004−5064. (d) Cukier, R. I.; Nocera, D. C. Proton-Coupled Electron Transfer. *Annu. Rev. Phys. Chem.* **1998**, *49*, 337−369. (e) Hammes-Schiffer, S.; Hatcher, E.; Ishikita, H.; Skone, J. H.; Soudackov, A. V. Theoretical Studies of Proton-Coupled Electron Transfer: Models and Concepts Relevant to Bioenergetics. *Coord. Chem. Rev.* **2008**, *252*, 384−394. (f) Mayer, J. M. Proton-Coupled Electron Transfer: A Reaction Chemist's View. *Annu. Rev. Phys. Chem.* **2004**, *55*, 363−390. (g) Costentin, C.; Robert, M.; Savéant, J.-M. Concerted Proton−Electron Transfers: Electrochemical and Related Approaches. *Acc. Chem. Res.* **2010**, *43*, 1019−1029. (h) Weinberg, D. R.; Gagliardi, C. J.; Hull, J. F.; Murphy, C. F.; Kent, C. A.; Westlake, B. C.; Paul, A.; Ess, D. H.; McCafferty, D. G.; Meyer, T. J. Proton-Coupled Electron Transfer. *Chem. Rev.* **2012**, *112*, 4016−4093.
(16) Bonin, J.; Costentin, C.; Robert, M.; Savéant, J.-M.; Tard, C. Hydrogen-Bond Relays in Concerted Proton-Electron Transfers. *Acc. Chem. Res.* **2012**, *45*, 372−381.
(17) Guérin, F.; McConville, D. H.; Vittal, J. J. Conformationally Rigid Diamide Complexes of Zirconium: Electron Deficient Analogs of Cp_2Zr. *Organometallics* **1996**, *15*, 5586−5590.

DOI: 10.1021/acs.inorgchem.8b03346
Inorg. Chem. 2019, 58, 3724−3731